Locking of Small Magnetic Islands by Error Field in T-10 Tokamak

N.V. Ivanov, A.M. Kakurin
National Research Centre «Kurchatov Institute», Moscow, Russia

1. Introduction

The T-10 tokamak experimental data on the dynamics of $m = 2$ mode in the presence of the intrinsic Error Field are presented. In addition to the well-known effect of the large magnetic island locking which takes place at mode amplitude higher than 10^{-3} T in the regime in question, a locking of sufficiently small magnetic islands is observed. If the amplitude exceeds a certain threshold level, the mode is in the state of an irregular rotation. If the amplitude is lower than the threshold level, the mode rotation stops. The experimental data are simulated with the TEAR code [1, 2] utilizing the model for the non-linear Rutherford tearing mode in rotating plasma in the presence of the Error Field. Unlike [3], deviations of magnetic island rotation velocity from the velocity of the resonant plasma layer are not neglected in this model.

2. Experimental Result

The experiments were carried out in the Ohmic regime with the following discharge parameters: the toroidal magnetic field $B_T = 2.4$ T, the discharge current $I_P = 240$ kA and the line-average plasma density $n_e \approx 1 \times 10^{19}$ m^{-3}. The minor radius of the plasma was $a = 0.27$ m. A tokamak regime which was characterized by the $m = 2$ mode with non-monotonically varying amplitude was chosen for this experiment. The $m = 2$, $n = 1$ harmonic of the Error Field can be estimated as $B_{EF} = 1.5 \cdot 10^{-4}$T at the plasma boundary.

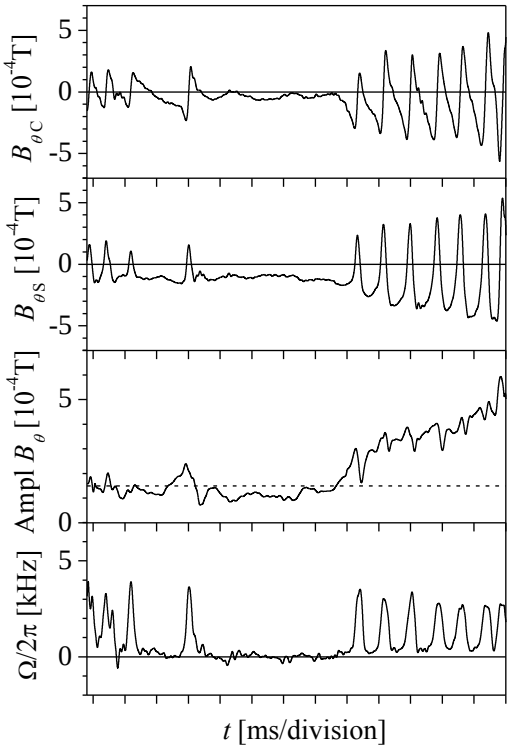

Fig. 1. Experimental waveforms of $m = 2$ mode cosine, $B_{\theta C}$, and sine, $B_{\theta S}$, components; mode amplitude, Ampl B_θ; instantaneous frequency of the mode, $\Omega/2\pi$

The space structure of the MHD mode was measured with a set of poloidal magnetic field sensors located at the inner side of the vacuum vessel wall. For each spatial Fourier harmonic with certain m and n numbers, the poloidal magnetic field perturbation at the radial position of the magnetic sensors is

$B_\theta(\theta, \varphi, t) = B_{\theta C}(t)\cos(m\theta - n\varphi) + B_{\theta S}(t)\sin(m\theta - n\varphi)$,

where φ and θ are the toroidal and poloidal angles, $B_{\theta C}(t)$ and $B_{\theta S}(t)$ are the cosine and sine components of the measured harmonic of the magnetic perturbation. The amplitude of the harmonic is $\mathrm{Ampl}B_\theta(t) = \sqrt{B_{\theta C}^2(t) + B_{\theta S}^2(t)}$. The space phase of this harmonic is defined as $\Phi(t) = \arctan\left[B_{\theta S}(t)/B_{\theta C}(t)\right]$ and the instantaneous value of the mode frequency is $\Omega(t) = \mathrm{d}\Phi/\mathrm{d}t$.

The experimental waveforms of the $m = 2$ mode signals in a case of the mode amplitude non-monotonic variation in time are shown in Fig. 1. If the mode amplitude exceeds the level of about Ampl $B_\theta = 1.5 \cdot 10^{-4}$ T, the mode is in a state of the irregular rotation. With a decrease of the amplitude lower than this threshold value the mode rotation pauses and recovers when the amplitude surpasses this level again. In the conditions of our experiment the observed threshold value of the amplitude corresponds to the calculated magnetic island width $W = 0.03$ m. Though in this paper we deal with relatively small magnetic islands, this width exceeds by an order of magnitude the level of transition to the Rutherford non-linear regime of the tearing mode [4].

3. Numerical modelling

The TEAR code is based on the non-linear Rutherford model [4 - 7] of the tearing mode. The effects of the plasma rotation and Resonant Magnetic Perturbation (RMP) are taken into account. As in [8, 9], in cylindrical approximation the equations

$$\frac{\partial}{\partial r}\left(r\frac{\partial \Psi_{\mathrm{C}}}{\partial r}\right)-\left(\frac{m^2}{r}+\frac{\mu_0 R}{B_{\mathrm{T}}}\frac{\partial j/\partial r}{\mu - n/m}\right)\Psi_{\mathrm{C}}+\mu_0\sum_{\mathrm{k}} r i_{\mathrm{k\,C}}\,\delta(r-r_{\mathrm{k}})=0\,, \qquad (1)$$

$$\frac{\partial}{\partial r}\left(r\frac{\partial \Psi_{\mathrm{S}}}{\partial r}\right)-\left(\frac{m^2}{r}+\frac{\mu_0 R}{B_{\mathrm{T}}}\frac{\partial j/\partial r}{\mu - n/m}\right)\Psi_{\mathrm{S}}+\mu_0\sum_{\mathrm{k}} r i_{\mathrm{k\,S}}\,\delta(r-r_{\mathrm{k}})=0 \qquad (2)$$

are used for the calculation of the radial distribution of the cosine, Ψ_{C} , and sine, Ψ_{S} , components of the helical magnetic flux perturbation:

$$\Psi = \Psi_{\mathrm{C}}(r,t)\cos(m\theta - n\varphi) + \Psi_{\mathrm{S}}(r,t)\sin(m\theta - n\varphi)\,. \qquad (3)$$

The poloidal and radial components of the magnetic field perturbation are $B_\theta = -\partial\Psi/\partial r$ and $B_{\mathrm{r}} = (1/r)\partial\Psi/\partial\theta$. We assume that $R >> a$, $m \geq n$. The solution of (1), (2) satisfies the boundary conditions $\Psi_{\mathrm{C,S}}(0) = \Psi_{\mathrm{C,S}}(b) = 0$, where $b = 0.5$ m is the effective radius of the perfectly conducting outer wall. In (1) and (2), i_{kC} and i_{kS} are the cosine and sine components of the external helical current surface densities at radii $r = r_{\mathrm{k}} \geq a$:

$$i_{\mathrm{k}} = i_{\mathrm{k\,C}}(t)\cos(m\theta - n\varphi) + i_{\mathrm{k\,S}}(t)\sin(m\theta - n\varphi)\,. \qquad (4)$$

In this paper we assume that the RMP is produced by two surface currents outside the plasma, including the current, $i_{1\,\mathrm{C,S}}$, which makes the permanent Error Field and the current with the surface density $i_{2\,\mathrm{C,S}} = -\sigma h \dfrac{\mathrm{d}\Psi_{\mathrm{C,S}}(r_{\mathrm{VV}})}{\mathrm{d}t}$, generated in the resistive vacuum vessel wall at $r = r_{\mathrm{VV}}$ due to the magnetic flux variations in time. In this formula, $h = 0.3\times10^{-3}$ m is the effective thickness of the vacuum vessel wall and σ is the stainless-steel wall conductivity.

The solution of the equations (1), (2) represent the superposition

$$\Psi_{\mathrm{C,S}}(r) = \Psi_{0\,\mathrm{C,S}}(r) + \Psi_{\mathrm{i\,C,S}}(r) \qquad (5)$$

of the solution $\Psi_{0\,\mathrm{C,S}}(r)$ of homogeneous equations with $i_{\mathrm{k\,C,S}} = 0$ and partial solutions $\Psi_{\mathrm{i\,C,S}}(r)$ of the non-homogeneous equations with $i_{\mathrm{k\,C,S}} \neq 0$ satisfying the boundary conditions $\Psi_{\mathrm{i\,C,S}}(r_{\mathrm{S}} + \mathrm{W}/2) = \Psi_{\mathrm{i\,C,S}}(b) = 0$, where $W = 4\sqrt{\left.\dfrac{R\sqrt{\Psi_{\mathrm{C}}^2+\Psi_{\mathrm{S}}^2}}{r_{\mathrm{S}}B_{\mathrm{T}}\,|\mathrm{d}\mu/\mathrm{d}r|}\right|_{r_{\mathrm{S}}}}$ is the width of the magnetic island, r_{S} is the radius of the magnetic surface on which $\mu(r_{\mathrm{S}}) = n/m$. The stability index of the tearing mode consists of the axisymmetric part $\Delta'_0(W)$ independent on the

external helical current and the part $\Delta'_{\mathrm{i\,C,S}}(W)$ proportional t o the components of the external helical current:

$$\Delta'_{\mathrm{C,S}}(W)=\frac{\Psi'_{\mathrm{C,S}}(r_{\mathrm{S}}+W/2)-\Psi'_{\mathrm{C,S}}(r_{\mathrm{S}}-W/2)}{\Psi_{\mathrm{C,S}}(r_{\mathrm{S}})}=\Delta'_{0}(W)+\Delta'_{\mathrm{i\,C,S}}(W), \tag{6}$$

where

$$\Delta'_{0}(W)=\frac{\Psi'_{0\mathrm{C}}(r_{\mathrm{S}}+W/2)-\Psi'_{0\mathrm{C}}(r_{\mathrm{S}}-W/2)}{\Psi_{0\mathrm{C}}(r_{\mathrm{S}})}=\frac{\Psi'_{0\mathrm{S}}(r_{\mathrm{S}}+W/2)-\Psi'_{0\mathrm{S}}(r_{\mathrm{S}}-W/2)}{\Psi_{0\mathrm{S}}(r_{\mathrm{S}})}, \tag{7}$$

$$\Delta'_{\mathrm{i\,C,S}}(W)=\frac{\Psi'_{\mathrm{i\,C,S}}(r_{\mathrm{S}}+W/2)}{\Psi_{0\,\mathrm{C,S}}(r_{\mathrm{S}})}. \tag{8}$$

In (6) – (8), Ψ' denotes dΨ/dr.

The time evolution of the cosine and sine components of the magnetic flux perturbation $\Psi_{\mathrm{C,S}}$ at the radius $r = r_{\mathrm{S}}$ is described by the modified Rutherford equations:

$$\frac{\mathrm{d}\Psi_{\mathrm{C}}}{\mathrm{d}t}=\pi a^2\omega_{\mathrm{R}}\left[\frac{\Delta'_0+\beta_{\mathrm{p}}\left(\Delta'_{\mathrm{BS}}-\Delta'_{\mathrm{GGJ}}-\Delta'_{\mathrm{pol}}\right)}{W}+\frac{\Delta'_{\mathrm{iC}}}{W}\right]\Psi_{\mathrm{C}}-\Omega_{\mathrm{nat}}\Psi_{\mathrm{S}}, \tag{9}$$

$$\frac{\mathrm{d}\Psi_{\mathrm{S}}}{\mathrm{d}t}=\pi a^2\omega_{\mathrm{R}}\left[\frac{\Delta'_0+\beta_{\mathrm{p}}\left(\Delta'_{\mathrm{BS}}-\Delta'_{\mathrm{GGJ}}-\Delta'_{\mathrm{pol}}\right)}{W}+\frac{\Delta'_{\mathrm{iS}}}{W}\right]\Psi_{\mathrm{S}}+\Omega_{\mathrm{nat}}\Psi_{\mathrm{C}}, \tag{10}$$

where $\omega_{\mathrm{R}}=1/\tau_{\mathrm{R}}$ is the inverse resistive time, $\tau_{\mathrm{R}}=\mu_0 a^2/\eta$. In (9), (10), the terms Δ'_{BS}, Δ'_{GGJ} and Δ'_{pol} are the bootstrap, curvature and polarization neoclassical terms respectively (see [10 - 12]). The saturation level of the magnetic island width W_{sat} is determined by the condition $\Delta'_0+\beta_{\mathrm{p}}\left(\Delta'_{\mathrm{BS}}-\Delta'_{\mathrm{GGJ}}-\Delta'_{\mathrm{pol}}\right)=0$.

In the equations (9), (10), $\Omega_{\mathrm{nat}}=mV_\theta/r_{\mathrm{S}}-nV_\varphi/R-\Omega_{e*}$ is the natural frequency depending on the poloidal, V_θ, and the toroidal, V_φ, rotation velocities of the resonant plasma layer $r_{\mathrm{S}}-W/2\le r\le r_{\mathrm{S}}+W/2$, as well as on the frequency of the electron diamagnetic drift, Ω_{e*}, [3, 7, 13 - 16]. In the TEAR code the equations of the resonant layer angular motion in the toroidal and poloidal directions are used to calculate the V_θ and V_φ time variations due to the interaction between the RMP and magnetic island structure (see [2]).

The result of the simulation for the conditions of our experiment is shown in Fig. 2. One can see, that the used numerical model in general features correctly describes the experimental data. The mode rotation stops after the decrease of the amplitude lower than a certain threshold value. The rotation recovers when the growing amplitude exceeds this level again. In the conditions under consideration,

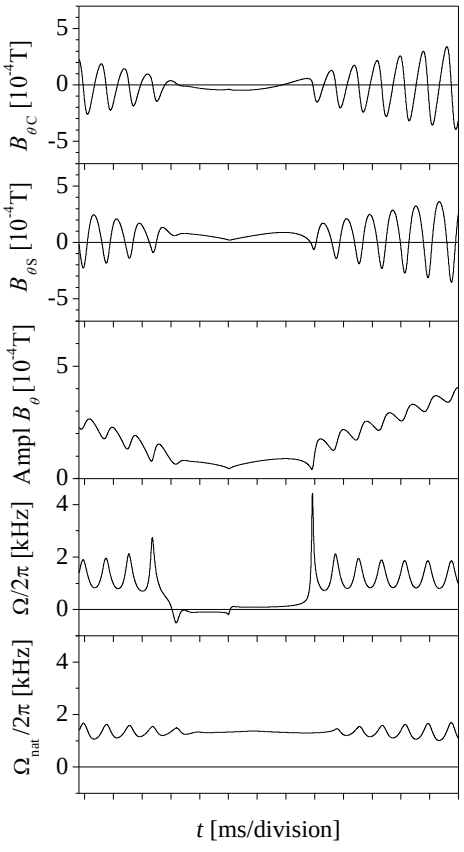

Fig. 2. Calculated waveforms of m = 2 mode cosine, $B_{\theta\mathrm{C}}$, and sine, $B_{\theta\mathrm{S}}$, components; mode amplitude, Ampl B_θ; instantaneous frequency, $\Omega/2\pi$ and natural frequency, $\Omega_{\mathrm{nat}}/2\pi$

the variations of the calculated natural frequency Ω_{nat} are small and do not explain the pause of mode rotation.

The explanation follows from the consideration of the equations (9), (10). Multiplying the equation (9) by Ψ_S, the equation (10) by Ψ_C and calculating the difference between these equations, one can obtain the instantaneous frequency of the mode:

$$\Omega = \frac{\mathrm{d}}{\mathrm{d}t}\left(\arctan\frac{\Psi_S}{\Psi_C}\right) = \Omega_{nat} - \frac{16\pi\omega_R a^2 R}{r_S B_T \left|\mathrm{d}\mu/\mathrm{d}r\right|}\frac{\sqrt{\left(\Psi'_{iS}\right)^2 + \left(\Psi'_{iC}\right)^2}}{W^3}\sin\left(\Phi_\Psi - \Phi_i\right) \qquad (11)$$

where $\Phi_\Psi - \Phi_i$ is the difference between the spatial phases of the tearing mode, $\Phi_\Psi = \arctan\frac{\Psi_S}{\Psi_C}$, and the RMP, $\Phi_i = \arctan\frac{\Psi_{iS}}{\Psi_{iC}}$. The variations of Ω with respect to the natural frequency Ω_{nat} are described by the second term in the right-hand-side of (11). These variations take place periodically along with the rotation of the mode relating to the RMP. The range of the second term variations is proportional to the RMP value and inversely proportional to W^3. It increases with the reduction of the magnetic island width. In the case of sufficiently small island width and appropriate phase difference, $\Phi_\Psi - \Phi_i$, the condition of the mode locking $\Omega = 0$ takes place. It should be noted that this condition does not directly depend on Δ'_0 and on the neoclassical terms in the modified Rutherford equations. As it can be estimated from (11), the mode locking occurs when the magnetic island width is less than the threshold value: $\frac{W}{a} \approx 5\left(\frac{R}{a}\frac{\omega_R}{\Omega_{nat}}\frac{B_{EF}}{B_T}\right)^{\frac{1}{3}}$. For our experimental conditions, this formula gives the estimation of the magnetic island width $W = 0.05$ m that roughly agree with the value obtained from the experiment. Even in the case of arbitrary small Error Field, the mode locking takes place for sufficiently small magnetic islands.

4. Summary

The experimental observation of the mode locking in the case of sufficiently small mode amplitude is observed. The explanation is attributed to the asymmetric effect of the Error Field on the tearing mode stability index.

References

1. Ivanov N.V., Chudnovskiy A.N., Kakurin A.M., Orlovskiy I.I. 33rd EPS Conference on Plasma Phys. Rome, 19 - 23 June 2006 ECA Vol.**30I**, P-1.176 (2006). http://epsppd.epfl.ch/
2. Ivanov N.V., Chudnovskiy A.N., Kakurin A.M., Orlovskiy I.I. 35th EPS Conference on Plasma Phys. Hersonissos, 9 - 13 June 2008 ECA Vol.**32D**, P-1.068 (2008). http://epsppd.epfl.ch/
3. Fitzpatrick R. Nucl. Fusion **33** (1993) 1049.
4. Rutherford P.H. Phys. Fluids **16** (1973) 1903.
5. Furth H.P., Rutherford P.H., Selberg H. Phys. Fluids **16** (1973) 1054.
6. White R.B., Monticello D.A., Rosenbluth M.N., et al. Phys.Fluids **20** (1977) 800.
7. Monticello D.A., White R.B. Phys. Fluids **23** (1980) 366.
8. Chudnovskiy A.N., Gvozdkov Yu.V., Ivanov N.V., Kakurin A.M., et al. Nucl. Fusion **43** (2003) 681.
9. Chudnovskiy A.N., Ivanov N.V., Kakurin A.M., Orlovskiy I.I., et al. Nucl. Fusion **44** (2004) 287.
10. Progress in the ITER Physics Basis, Chapter 3. Nucl. Fusion **47** (2007) S128.
11. Sauter O., La Haye R.J., Chang Z., et al. Phys. Plasmas **4** (1997) 1654.
12. Mikhailovskii A.B. Contrib. Plasma Phys **43** (2003) 125.
13. Yu Q., Guenter S., Kikuchi Y., Finken K.H. Nucl. Fusion **48** (2008) 024007.
14. Kikuchi Y., Finken K.H., Jakubowski M., et al. PPCF **48** (2006) 169.
15. Hosea J.C., Jobes F.C., Hickok R.L., Dellis A.N. Phys. Rev. Letters **30** (1973) 839.
16. Koslowski H.R., Liang Y., Kramer-Flecken A., et al. Nucl. Fusion **46** (2006) L1.